Gupta et al. Scr Med. 2026 May-Jun;57(3):489-503. DOI:10.5937/scriptamed57-60631

ORIGINAL ARTICLE

Retinoic Acid Delivery via Ultraflexible Nanovesicular System for the Management of Posterior Segment Ocular Diseases

Vandana Gupta,[1] Noopur Srivastava,[2] Megha Verma,[3] Mahima Beohar,[3] Vishal Verma[3]

1. Department of Pharmaceutical Sciences, Shalom Institute of Health and Allied Sciences, Sam Higginbottom University of Agriculture, Technology and Sciences (SHUATS), Naini, Prayagraj, Uttar Pradesh, India.
2. The Oxford College of Pharmacy, Rajiv Gandhi University of Health Sciences, Bengaluru, Karnataka, India.
3. Department of Pharmacy, Gyan Ganga Institute of Technology and Sciences, Tilwara Ghat, Jabalpur, Madhya Pradesh, India.

Citation:
Gupta V, Srivastava N, Verma M, Beohar M, Verma V. Retinoic acid delivery via ultraflexible nanovesicular system for the management of posterior segment ocular diseases. Scr Med. 2026 May-Jun;57(3):489-503.

Corresponding author:
VANDANA GUPTA
E: vandana.gupta@shiats.edu.in

Abstract

Background/Aim: Ophthalmic diseases, especially conditions of posterior segment of eye encompass a range of conditions affecting the vitreous, choroid and retina, resulting in both structural and functional deficiencies in the eye. This study aimed to formulate and evaluate ultraflexible nanovesicular systems (nano-transfersomes) for local delivery of retinoic acid to the deeper posterior regions of the eye.

Methods: Transfersome compositions were optimised and characterised for vesicle size and distribution, surface charge (zeta potential), encapsulation efficiency, surface morphology, viscosity and pH. Additional evaluations included in vitro drug release in simulated tear fluid (STF), three-month stability testing, and ocular safety assessment using the hen's egg chorioallantoic membrane (HET-CAM) test.

Results: The optimised formulation (F12) had a mean vesicle diameter of 155.32 ± 4.45 nm, measured by dynamic light scattering (Malvern Zetasizer ZEM 5002, UK). The zeta potential was approximately –36.5 mV, indicating a negative surface charge and reduced particle aggregation. Entrapment efficiency across formulations ranged from 65.45 ± 1.27 % to 79.12 ± 2.23 %. Nano-transfersomes exhibited spherical, elastic morphology with uni- or multilamellar vesicle structures. Viscosity of the retinoic acid–loaded formulations ranged from 20.0 ± 2.1 to 48.0 ± 1.8 cP, and pH ranged from 5.0 ± 0.5 to 7.0 ± 0.1. In STF, cumulative drug release reached 98.89 ± 0.45 % after 24 h.

Conclusion: Retinoic acid–loaded ultraflexible nano-transfersomes demonstrated a sustained release profile and greater stability under refrigerated conditions. The formulation showed suitable physicochemical properties for ocular application and may offer a promising approach to deliver retinoic acid to the posterior segment of the eye, owing to its flexibility, prolonged release and small size.

Key words: Tretinoin; Exosomes; Ultraflexible nanovesicular system; Posterior eye; Diseases, ocular.

Received: 5 August 2025
Revision received: 29 August 2025
Accepted: 29 August 2025

Introduction

Ophthalmic diseases, especially conditions of posterior segment of eye encompass a range of conditions affecting the vitreous, choroid and retina, resulting in both structural and functional deficiencies in the eye.[1-4] The case of optic disorders escalate rapidly owing to diabetes melli-

tus, an aging demographic and various lifestyle factors.[5-8] These conditions profoundly affect patients' visual experiences and standard of life, become a major public health concern.[9]

The cure typically employed as remedy for dorsal regions of the optic predominantly consists of Lumitin therapies, in addition to glucocorticoids and antioxidants.[10] Further, periocular and intraocular injections are the alternative strategies, can more accurately focus on the impacted area and provide extended drug efficacy.[11] However, these techniques are associated with certain disadvantages, including discomfort, non-invasiveness as well as the potential for infection and haemorrhage. The most prevalent method for addressing ocular conditions is through the topical administration.[12, 13] Nevertheless, these medications frequently face challenges in effectively penetrating the deeper tissue layers at the site of the lesion due to the ocular physiological and anatomical barriers.[14, 15]

Ultraflexible nanovesicular system, a form of flexible liposomal system, showcases an innovative strategy for administering medicament in posterior region of ocular diseases, specifically for conditions that struggle with inadequate absorption through the ocular physiological and anatomical hurdles.[16-19] By enhancing drug penetration and prolonging its retention at the target location, nano-transfersomes can enhance treatment effectiveness and minimise the necessity for invasive techniques such as intravitreal injections.[20-22] Additionally, retinoic acid is a derivative of a class of lipid-soluble compounds that exhibit improved permeability across the ocular barrier.[23] It traverses various barriers within the eye, including the blood-retina barrier (BRB), by employing specific transporters and mechanisms.[24] This examination focuses on forming and assessing the localised nano-transfersome drug carrier made of retinoic acid, designed for treating posterior region ocular ailments.

Methods

Retinoic acid was attained as gift sample from pharmaceutical company and soya phosphatidyl choline (PC) was bought from *Himedia Laboratory*, Mumbai. Ethanol, chloroform from *CDH Chemical* Pvt Ltd. New Delhi. Dialysis membrane of Mol. Wt. cutoff 1200 was bought from *Himedia Laboratory*, Mumbai. Double distilled water was processed newly and used whenever required. Rest of the various reagents and compound directed were of analytical grade.

Preparation of retinoic acid loaded nano-transfersomes

The appropriate quantity of soya PC, retinoic acid and surfactant (span 20) were taken in flask, after that ethanol was added with manual shaking. The formation of thin film took place by using a rotary evaporator for 15 minutes at 25 °C, with a pressure of 600 mm Hg at a spin rate of 100 rpm. Subsequently, the liquid was separated in the presence of nitrogen gas.[25] The film was set in a desiccator for a minimum of 12 h to discard remaining solvent, later film was hydrated with the prepared 10 ml of simulated tear fluid (STF) pH 7.4, through simple oscillation for 30 min. Following this, the mixture was stirred for an additional 30 min. using an orbital shaker. The nano-transferosomes were then examined under a microscope. The nano-transferosomal suspension containing retinoic acid was stored in a refrigerator at 4 ^{0}C until characterisation.

Refining of nano-transfersomes

The refining of the transferosomal composition carrying retinoic acid was done by adjusting distinct composition and method parameters, such as the lipid to surfactant ratio, ethanol volume, retinoic acid quantity and stirring duration. A range of formulations (F1-F14) was developed utilising these parameters and refined upon the average vesicle diameter and percentage entrapment capacity.[26]

In vitro examination of retinoic acid loaded nano-transfersomes

Vesicle size, size distribution and surface charge
The vesicles diameter, arrangement and its exterior charge were estimated using the Photon Correlation Spectroscopy (PCS) technique (Malvern Zeta master, ZEM 5002, *Malvern*, UK). The Zeta potential of the Nano-transfersomes was determined based on the Helmholtz–Smoluchowsky equation, interpreted from their electrophoretic mobility. To evaluate the vesicle diameter, distribution and Zeta potential, various formulations of retinoic acid-filled nano-transfersomes were diluted with a 0.9 % NaCl solution. The hydrated formulation was then placed into a cataphoretic cuvette for Zeta potential measurement.[27]

Percentage entrapment capacity (% EC)

To find out the entrapment capacity, a 10 mL suspension of retinoic acid-loaded nano-transfersomes by centrifuging at 15,000 rpm for one hour, facilitating the parting of the deceived drug from the unentrapped portion as a result clear phase discard from the unentrapped drug, the settled material containing the entrapped drug was lysed by methanol and thereafter analysed through UV spectrophotometer (Labindia 3000+) at a wavelength (λ_{max}) of 282 nm and percent of retinoic acid within the formulation was calculated by below equation:[28]

$$\% \text{ EC} = \frac{\text{Therotical drug content - Practical drug content}}{\text{Therotical drug content}} \times 100$$

The total amount of retinoic acid, represented as practical drug content, was derived from the quantity present in both the supernatant and sediment.

In vitro drug release study

The best nano-transfersome composition (F12) was selected for study, performed by dialysis diffusion technique with a dissolution test apparatus. The dissolution medium employed was artificial tears fluid (ATF) with a pH of 7.4 in which cellulose acetate membrane molecular weight cut-off of 12,000–14,000 was utilised for the dialysis process, ensuring the drug's permeation while retaining the nano-transfersomal vesicles. Prior to use, the membrane was immersed in ATF for 12 h. A volume of 4 mL of the nano-transfersomal dispersion was introduced into a glass cylinder measuring 8 cm in length and 1 cm in diameter, with the dialysis membrane secured at the opening of the cylinder using a thread. Each glass cylinder was linked with the shaft of the dissolution tester (USP Dissolution Tester, Labindia DS 8000) and submerged into a 50 mL beaker containing 10 mL of ATF as the dissolution medium, ensuring it did not reach the base of the beaker. The beakers were subsequently placed in the dissolution tester liner, which contained approximately 100 mL of water to maintain a temperature of 37 ± 0.5 °C. The glass cylinders were set to rotate at a consistent speed of 20 rpm. At specified time intervals (0, 1, 2, 3, 4, 5, 6, 7, 8, 9, 10, 11 and 24 h); 1 mL of the dissolution medium was extracted. The samples were replaced with fresh dissolution medium to maintain constant volume. Drug concentrations in samples were analysed using spectrophotometrically at wavelength of drug 282 nm. The release experiments were carried out in triplicates and the mean ± SD were recorded. During each sampling interval, samples are withdrawn and replaced by equal volumes of fresh receptor fluid on each sampling.[29]

Various kinetics approaches were employed to find the results, elucidating the extricate process. The zero-order rate kinetics featuring where the medication extricates frequency is free of its concentration. Conversely, the first-order kinetic pertains to systems where the medication extricate frequency is subject on concentration. Higuchi articulated that medication extricate from an insoluble matrix follows a time-dependent method described by the square root of time, based on Fickian diffusion. Additionally, Korsmeyer et al established a straight forward mathematical relationship that describes medication extricate from a polymeric system.[30]

Surface morphology by transmission electron microscope (TEM)

The most effectively optimised formulation (F12) of an ultraflexible nanovesicular system containing retinoic acid was diluted to a ratio of 100:1, applied to a copper 300-mesh grid for duration of 15 minutes and subsequently fixed using glutaraldehyde for 3 minutes. After washing, the samples were stained with a lead citrate solution for 3 minutes. Imaging was conducted using a JEOL JEM F-200 electron microscope from Japan at a magnification of 100,000 times.[31]

Measurement of viscosity and pH

The flow characteristics of the retinoic acid-loaded ultraflexible nanovesicular formulations were assessed using a Brookfield viscometer (*Brookfield Engineering Laboratories*, Stoughton, MA, United States, with software) and a small sample adapter (spindal and chamber SC4-18/13R) between the percentage torque values of 10 to 100.[32] Using a pH indicator (Eutech waterproof pHTestr® 10), the pH range of the retinoic acid contained in different ultraflexible nanovesicular composition was measured directly in samples at room temperature (37 ^{0}C ± 2 ^{0}C).[33]

Stability studies

Drug-loaded nano-transfersomes F12 formulation was subjected to a stability investigation for three weeks at two distinct temperatures: room temperature (25–28 °C ± 2 °C) and refrigeration temperature (4.0 °C ± 0.2 °C). To inhibit any interaction between the composition and the con-

tainer's glass, the formulation that was the topic of the stability investigation was kept in a borosilicate container. The following equation and the UV Visible Spectrophotometer (Shimadzu 1900 Japan) were used to analyse the formulations for drug concentration (% DC) and further for any physical changes and vesicular size using (Malvern Zetamaster, ZEM 5002, *Malvern*, UK) weekly up to 3 weeks. Formulation was examined three times and the average value was calculated as the outcome.[34]

$$\% DC = \frac{\text{Concentration x Dilution factor x Volume of formulation}}{\text{Total amount of drug added}}$$

Ocular irritation/tolerance test (Hühner-Embryonen-Test: HET)

The HET, referred to as the hen's egg test on chorioallantoic membrane (HET-CAM), serves as an appropriate alternative to animal testing (Draise test). In this method sample is implemented on the CAM, where responses such as haemorrhage, intravascular coagulation, or ruptured blood vessels are evaluated microscopically over a specified time limit.[35] Above sensitisation happened after the mucosal administration of the sample, applied directly to the CAM of a hen's egg. In order to conduct the test, fertilised eggs from *Gallus domesticus,* aged 10 days, were incubated for duration of 24 hours at a temperature of 37.5 °C and a relative humidity of 55 %. Further, the eggshell and the inner membrane of chicken eggs were removed in advance, allowing the CAM that separates the embryo from the air chamber to be visible. Two groups were utilised to ascertain the irritation score (IS). Each group comprised of 3 chicken eggs. One group assigned for the positive controls (internal standard) and another group was assigned as treated group. A solution of 0.1 N NaOH in distilled water, recognised for its irritative characteristics, was utilised as a reference point (positive controls) for assessing the potential for irritation. An equivalent of 0.05 % retinoic acid containing ultraflexible nanovesicular formulation (F12) was administered to the CAM. Following a 5-minute exposure, the membrane was washed with 5 mL of isotonic NaCl solution and the intensity of each reaction (n = 3) was documented. The duration in seconds for the onset of haemorrhage (*h*), lysis (*l*), or coagulation (*c*) was recorded and expressed as ocular irritation index (OIIs). The ocular irritation index [OII] was determined[36] using the following formula:

$$OII = \frac{(301-h) \times 5}{300} + \frac{(301-h) \times 7}{300} + \frac{(301-h) \times 9}{300}$$

The subsequent classification has been established: OII ≤ 1.0 was categorised as slightly irritating; 1.0 < OII ≤ 5.0 was deemed moderately irritating; 5.0 < OI I ≤ 9.0 was classified as irritating; and 9.0 < OII ≤ 21 was considered severely irritating.

Statistical analysis

The data obtained were displayed as the mean ± standard deviations (SD) utilising Excel software and SPSS version 27. All experiments were conducted in triplicate (n = 3). Significance was established as $p \leq 0.05$ following the execution of Student's t-test and ANOVA.

Results

Preparation and optimisation of retinoic acid containing nano-transfersomes

A number of retinoic acid-loaded nano-transfersomes (F1-F14) were produced using a modified lipid film hydration technique. In the current study, Span 20, similar to other edge activators, functioned as an edge modulator, decreasing the interfacial tension between the lipid bilayer of the nano-transfersome and the surrounding environment.[37] This reduction enhances the flexibility of the vesicles, enabling them to navigate through ocular barriers and deliver the drug to deep layers of eye. Phosphatidyl choline, utilised in the formulation of nano-transfersomes, is a phospholipid that inherently self-assembles into vesicles in aqueous environment, thereby creating the bilayer structure characteristic of transfersomes.[38] This phospholipid enhances drug encapsulation, improves penetration and facilitates drug delivery particularly for the posterior segment of the eye. Moreover, ethanol functions as a co-solvent, assisting in the solubilisation of lipids and serving as a permeation enhancer, thereby augmenting the ocular permeability to pharmaceuticals by traverse the anatomical barriers of the eye to access the posterior segment.[39] This disturbance promotes the penetration of drug molecules into and through the stratum corneum, the outermost layer of the cornea, along with the conjunctiva, enables the nano-transferosomes to enter the eye. Retinoic acid is a hydrophobic substance and nano-transfersomes, due to their lipid-based structure can enhance the solubility of retinoic acid, enabling a greater concentration

Table 1: Optimisation studies: Optimisation of the retinoic acid-loaded nano-transfersomes has been carried out by adjusting the lipid to surfactant ratio, the volume of ethanol, the concentration of retinoic acid and the duration of stirring and responses were observed in terms of entrapment efficiency and vesicular size

Composition code	Soya PC: Span 20 (% w/v)	Ethanol (mL)	Medicament (% w/v)	Average vesicle diameter (nm)	% entrapment capacity
F1	0.5 : 0.5	10	1.0	225.65 ± 5.15	71.65 ± 2.22
F2	1.0 : 0.5	10	1.0	185.65 ± 4.22	75.23 ± 2.56
F3	1.5 : 0.5	10	1.0	298.85 ± 6.43	69.98 ± 2.12
F4	2.0 : 0.5	10	1.0	265.74 ± 5.45	65.85 ± 3.23
F5	2.0 : 0.5	5	1.0	212.25 ± 4.89	76.58 ± 3.28
F6	2.0 : 0.5	10	1.0	185.65 ± 4.48	74.65 ± 2.28
F7	2.0 : 0.5	15	1.0	225.65 ± 4.97	69.98 ± 1.98
F8	2.0 : 0.5	20	1.0	268.98 ± 5.45	65.45 ± 1.27
F9	2.0 : 0.5	10	1.0	165.45 ± 4.58	78.12 ± 1.65
F10	2.0 : 0.5	10	1.5	215.56 ± 5.16	65.56 ± 2.26
F11	2.0 : 0.5	10	2.0	241.32 ± 5.38	67.85 ± 3.23
		Stirrer time (min)			
F12*	**1.5 : 1.0**	**30**	**1.0**	**155.32 ± 4.45**	**79.12 ± 2.23**
F13	2.0 : 1.0	20	1.0	178.86 ± 5.21	63.32 ± 2.18
F14	2.5 : 1.0	10	1.0	189.98 ± 4.37	54.47 ± 1.55

**Best optimised retinoic acid-loaded nano-transfersome formulation;*

to be delivered. Table 1 presents the optimisation parameters and responses regarding % EC and vesicle size for all evaluated experimental trials. It was noted that a higher ratio of lipid and an extended stirring duration in the experimental trials resulted in increased entrapment capacity (% EC) and a decrease in vesicular size during the optimisation study as observed for F12 formulation. It could be due to the increased volume of lipids available for encapsulating the substantial quantity of the drug.[40] Further, the act of stirring generates shear forces that can break apart larger vesicles, leading to a smaller and more uniform distribution of particle sizes.

Investigation of vesicle size, size distribution, polydispersity index (PDI) and surface charge

The size of the particles was significantly affected by the quantity of lipid utilised, ranging from 155.32 ± 32 nm to 298.85 ± 6.43 nm as the concentration of phospholipid increased. The optimised formulation, specifically F12, exhibited a particle size of approximately 155.32 ± 4.45 nm (Figure 1). These findings can be elucidated through the principles of PCS technique. PCS assesses Brownian motion, which is directly related to particle size. Typically, PCS focuses on measuring particles suspended in a liquid medium, where the diffusion rate of particles is influenced by their size; smaller particles diffuse more rapidly while larger particles do so at a slower rate. This measurement is achieved by analysing the fluctuations in the intensity of scattered light, detected through an appropriate optical setup.[41] Moreover, Figure 1 indicates the value of low PDI i.e. 0.393 for the optimised retinoic acid loaded nano-transfersome (F12). A low PDI of nano-transfersomes is essential for maintaining homogeneity and stability,[42] being integral part for enhancing medicament administration. This boosts both stability and drug entrapment, ultimately promoting efficient medicament administration to the posterior region of optic. The dimensions of the nano-transfersomes, which are directly associated with PDI, can influence their capacity to traverse the posterior region of optic, thus being intended target for medicament administration. The capacity of nano-transfersomes to engage with the retina and other posterior structures is contingent upon their surface properties, such as Zeta potential. Surface charge, also known as Zeta potential (ξ-potential) of the best composition (F12) was found to be -36.5 mV (Figure 2).

Assurance of % EC

The captured capacity of the best composition (F12) was observed to be 79.12 ± 2.23 %. The ideal concentration of phospholipid, combined with span-20 (a lipophilic surfactant), is essential for effective drug encapsulation, as these components create the vesicle membrane. Retinoic

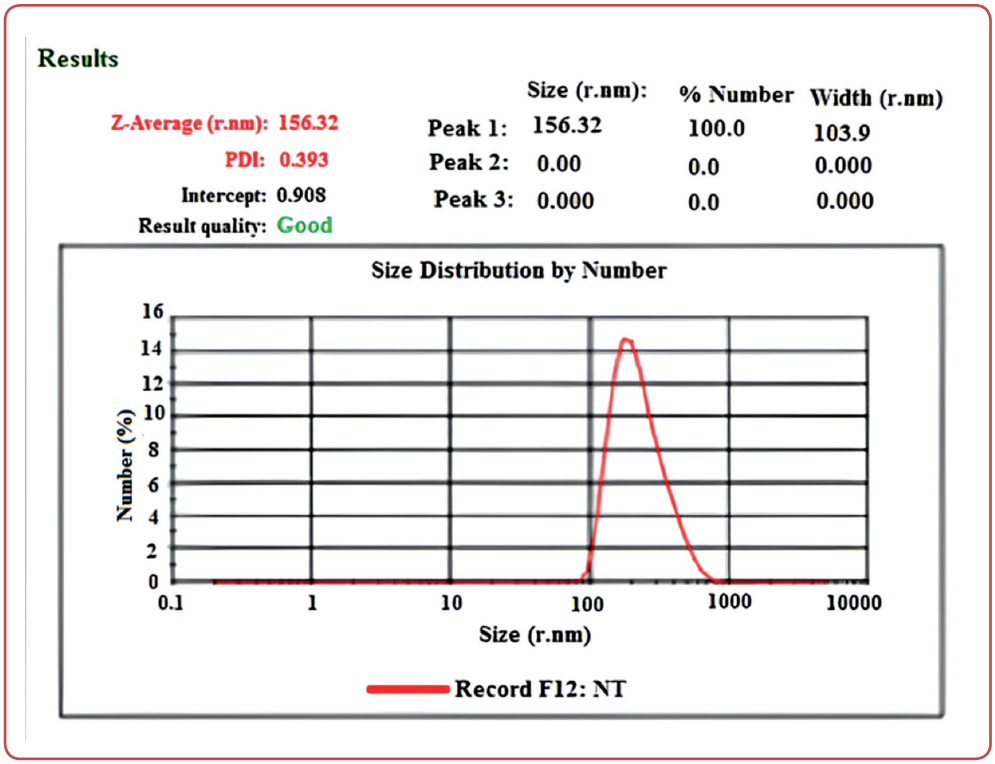

Figure 1: *Average particle size and size distribution curve of optimised formulation F12 along with value of PDI*

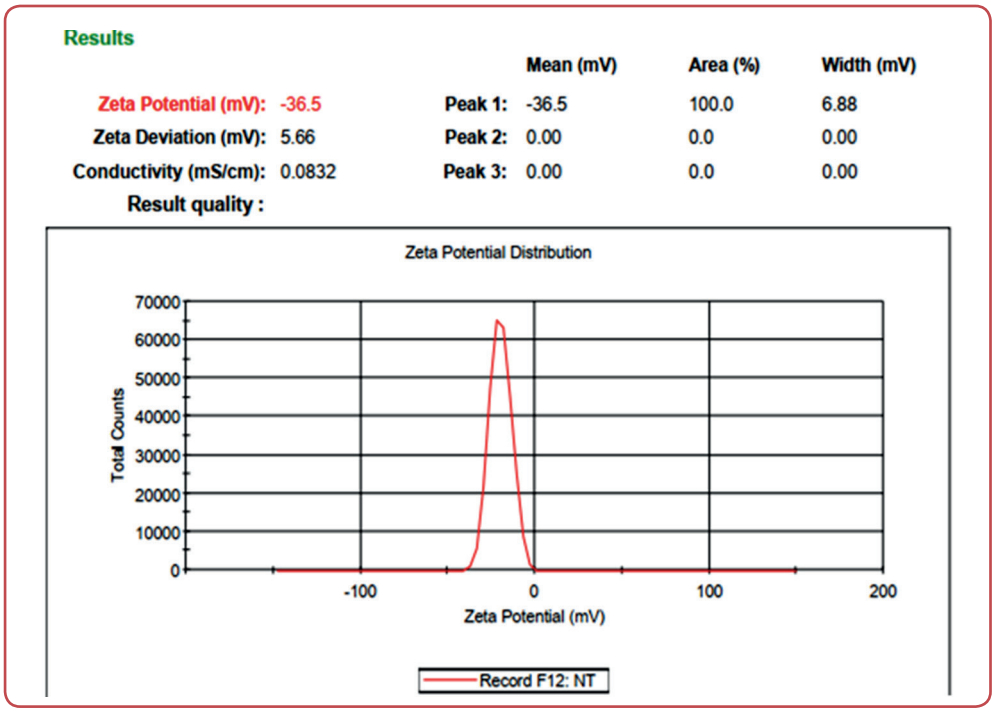

Figure 2: *Mean Zeta potential results and curve of Zeta potential of optimised formulation F12*

acid, which is a hydrophobic drug, can typically be integrated into the phospholipid bilayer of the nano-transfersome due to its capacity to partition into and remain within the lipid membrane. This partitioning process improves entrapment efficiency and safeguards the drug against degradation. It was noted that (Table 1) lower levels of ethanol can enhance entrapment by minimising vesicle size and boosting stability; however, excessive ethanol may result in lipid layer leakage and reduced entrapment. Additionally, prolonged stirring times of 10, 20 and 30 minutes were noted to result in slight increases in entrapment, with values of 54.47 ± 1.55 %, 63.32 ± 2.18 % and 79.12 ± 2.23 %, respectively.

In vitro medicaments extricate profiling

The *in vitro* retinoic acid release investigations were conducted on the optimised nano-transfersomal formulation i.e. F12 (Table 2). The data from the medicament extricate indicated the release of 12.25 ± 0.45 %, 19.98 ± 0.65 %, 26.65 ± 0.32 %, 32.25 ± 0.41 %, 41.15 ± 0.78 %, 48.89 ± 0.95 %, 55.65 ± 0.62 %, 65.58 ± 0.71 %, 72.32 ± 0.36 %, 88.56 ± 0.21 %, 92.65 ± 0.24 % and 98.89 ± 0.45 % at the 1, 2, 3, 4, 5, 6, 7, 8, 9, 10, 11 and 24 h of the study period, respectively.

The release profile of retinoic acid from nano-transferosomes has been demonstrated to exceed only 40 % within a period of 6 h exhibited prolonged drug release while around the 98 % of the drug was released within 24 hours (Table 2) from a nano-transferosome drug delivery system demonstrates a swift and effective drug release profile. This biphasic release pattern may prove especially beneficial for administering medications to the posterior segment of the eye, where prolonged release is frequently required for managing conditions such as diabetic retinopathy and age-related macular degeneration.

Table 2: In vitro medicament extricates of best F12 nano-transfersome composition

S No	Time (h)	Cumulative medicament extricate (%) (Mean ± SD)
1	0	00.00 ± 0.00
2	1	12.25 ± 0.45
3	2	19.98 ± 0.65
4	3	26.65 ± 0.32
5	4	32.25 ± 0.41
6	5	41.15 ± 0.78
7	6	48.89 ± 0.95
8	7	55.65 ± 0.62
9	8	65.58 ± 0.71
10	9	72.32 ± 0.36
11	10	88.56 ± 0.21
12	11	92.65 ± 0.24
13	24	98.89 ± 0.45

In vitro drug transport kinetics data analysis

Kinetic values for drug release have been produced to facilitate the application of mathematical models in the release kinetics of an optimised nano-transfersome formulation loaded with retinoic acid (F12). For example, data including the square root of time, logarithmic time, cumulative drug release (%), logarithmic cumulative drug release (%), cumulative drug remaining (%) and logarithmic cumulative drug remaining (%) has been generated (Table 3) to create graphs for the zero order, first order, Higuchi model and Korsmeyer–Peppas model.

To assess the drug release according to zero-order kinetics, a graph was created for optimised formulation (F12) illustrating the relationship between time and cumulative drug release percentage (Figure 3). The correlation coefficient (R^2) for the zero-order drug release kinetics was determined to be 0.763, indicating a moderate level of fit. This suggests that the model employed is effective in capturing the trend of drug release from the nano-transfersome. It implies that approximately 76.3 % of the variability in cumulative drug release can be accounted for by the selected model, while the remaining 23.7 % is attributed to other factors or variations not included in the model. Based on the graph, it can be concluded that the drug release did not adhere to zero-order release kinetics, as evidenced by the moderate to lower value.

According to first-order drug release kinetics, the rate of drug release is directly proportional to the concentration of the drug.[43] This implies that a higher concentration of the drug results in a correspondingly higher release rate, while a decrease in drug concentration leads to a reduction in the release rate. To investigate the first-order release kinetics of the nano-transfersome formulation (F12), a graph was created plotting the logarithm of the percentage of drug remaining against time (Figure 4). From the graph presented, it can be inferred that the drug release closely adheres to first-order release kinetics, as evidenced by a high R^2 value of 0.942.

Table 3: Mathematical treatment of in vitro medicament extricates for F12 nano-transfersome composition

Time (h)	Square root of time (√h)	Log time	Cumulative medicament extricate (%)	Log cumulative medicament extricate (%)	Cumulative medicament residual (%)	Log cumulative medicament residual (%)
1	1.000	0.000	12.25	1.088	87.750	1.943
2	1.414	0.301	19.98	1.301	80.020	1.903
3	1.732	0.477	26.65	1.426	73.350	1.865
4	2.000	0.602	32.25	1.509	67.750	1.831
5	2.236	0.698	41.15	1.614	58.850	1.770
6	2.449	0.778	48.89	1.689	51.110	1.709
7	2.645	0.845	55.65	1.745	44.350	1.647
8	2.828	0.903	65.58	1.817	34.420	1.537
9	3.000	0.954	72.32	1.859	27.680	1.442
10	3.162	1.000	88.56	1.947	11.440	1.058
11	3.316	1.041	92.65	1.967	7.350	0.866
24	4.898	1.380	98.89	1.995	1.110	0.045

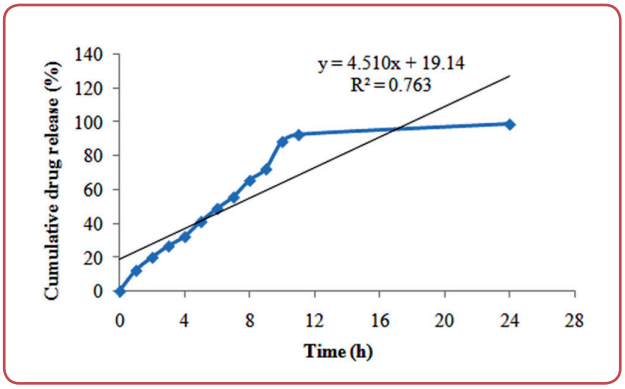

Figure 3: In vitro zero order release kinetic for optimised formulation (F12)

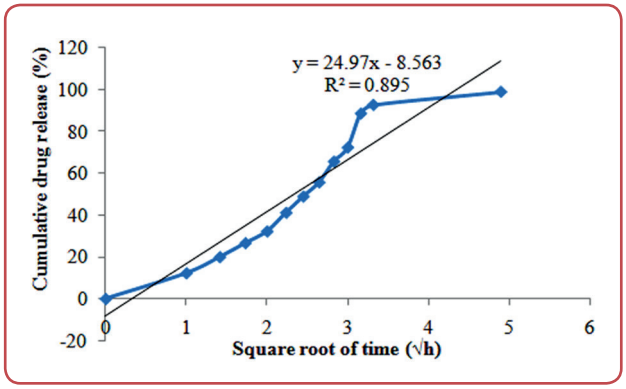

Figure 5: In vitro Higuchi model release kinetic for optimised formulation (F12)

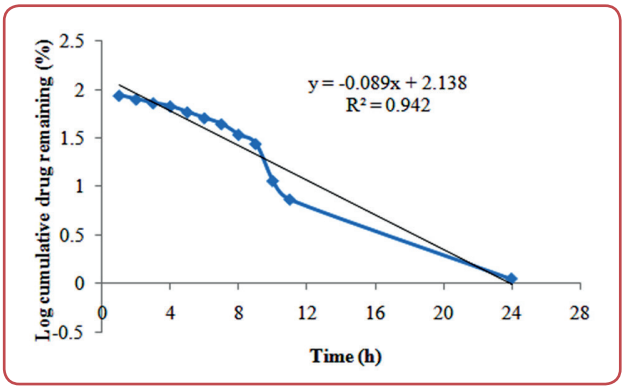

Figure 4: In vitro first order release kinetic for optimised formulation (F12)

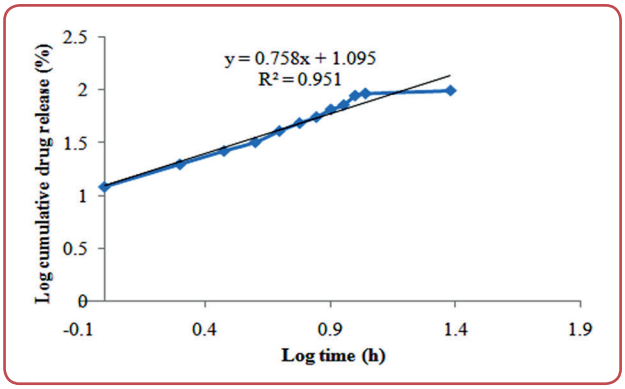

Figure 6: In vitro Krosmeyer - Peppas model release kinetic for optimised formulation (F12)

To examine the Higuchi model of drug release kinetics for the formulated F12 nano-transfersome, a graph was created illustrating the relationship between cumulative percentage of retinoic acid release and the square root of time (Figure 5). A high correlation coefficient indicates that the drug release mechanism is likely diffusion-based. The Higuchi model characterises drug release from a matrix system, especially when diffusion is the primary mechanism.[44] The graph suggested

Table 4: Regression (R2) evaluation information of nano-transfersomal composition F12

Optimised formulation	Zero order	First order	Higuchi's model	Korsmeyer-Peppas model
	R^2	R^2	R^2	R^2
F12	0.763	0.942	0.895	0.951

that the drug release is closely aligned with Higuchi drug release kinetics, as evidenced by a significant value. This indicates that approximately 89.5 % of the variability in drug release can be accounted for by the Higuchi model. Although it is not a perfect fit, a value of R^2 = 0.895 is still regarded as relatively high, implying that the Higuchi model serves as a credible framework for elucidating the drug release mechanism, which likely involves diffusion from a matrix system.

The Korsmeyer-Peppas approach, which is a power law model, serves as a mathematical framework for describing drug release, especially in controlled release situations. It examines the kinetics of medicament extricate by taking into account both diffusion and erosion processes.[45] To investigate the medicament extricate kinetics through Korsmeyer–Peppas model, a graph was created plotting log cumulative drug release percentage against log time. From the graph presented (Figure 6), it can be inferred that the medicament release closely adheres to Korsmeyer-Peppas drug release kinetics, as evidenced by the highest correlation coefficient value (R^2 = 0.951). Additionally, the Korsmeyer-Peppas model's R^2 value of 0.951 suggested a strong fit of the model to the drug release data, indicating that the action of medicament extricate which was likely controlled by diffusion, with possible contributions from the erosion or swelling of the polymer matrix.

A suitable mathematical model for the study of *in vitro* drug release was identified based on the highest correlation coefficient value. The *in vitro* drug release profile of retinoic acid embedded in nano-transfersomes was fitted to four distant mathematical approaches and assessed using the correlation coefficient R^2. The outcomes of all four models are presented in Table 4.

Transmission electron microscopic appearance of nano-transfersome

The images obtained indicated that nano-transfersomes loaded with retinoic acid exhibited spherical, oval and elongated shapes, appearing as multilamellar bilayer vesicles (Figure 7). The

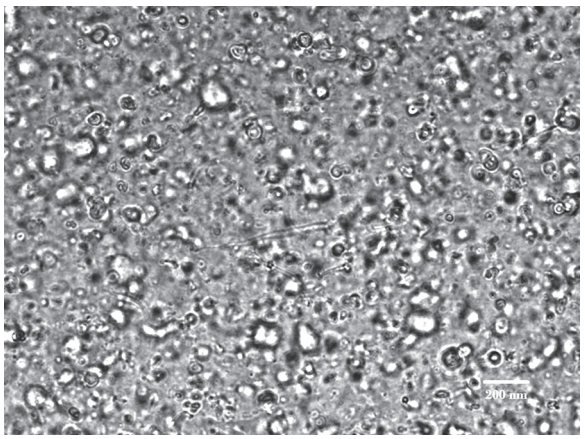

Figure 7: Transmission electron microscope (TEM) image of optimised nano-transfersome formulation F12 at a magnification of 100,000x

nano-transferosomes presented a consistent system of unique, nearly spherical particles characterised by smooth surfaces and loose aggregates, maintaining their spherical shape even under the challenging conditions of TEM analysis. Furthermore, the measured size corresponded with the results acquired through PCS. These images confirmed the successful formulation of nano-transfersomes.

Viscosity and pH measurement

Nano-transfersomes, which are flexible vesicles, must have an appropriate viscosity to ensure effective application and retention on the ocular surface, while also maintaining a physiological pH to prevent irritation and guarantee drug stability. The viscosity measurements of the retinoic acid-loaded nano-transfersome formulations (F1-F12) are presented cp in Table 5, revealing a range from 20.0 ± 2.1 to 48.0 ± 1.8 cP. It was noted that an increase in lecithin concentration typically results in higher viscosity, as evidenced by formulations F12 to F14, which, having a greater ratio of phosphatidyl choline, exhibited viscosity values of 45.9 ± 1.2 to 48.0 ± 1.8. Additionally, surfactants, functioning as edge activators, can enhance viscosity by forming micellar aggregates, thereby creating a denser network. The pH level of the retinoic acid-loaded nano-transfer-

some formulation must be assessed to ensure its suitability for ocular applications. The pH values for all retinoic acid-loaded nano-transfersome formulations, specifically F1-F14, varied from 5.0 ± 0.5 to 7.0 ± 0.1, as illustrated in Table 5.

Table 5: Viscosity and pH of different retinoic acid loaded nano-transfersome formulations ie F1-F14

Formulation code	Viscosity at 37 °C ± 2 °C (cP) (Mean ± SD)	pH (Mean ± SD)
F1	20.0 ± 2.1	6.6 ± 0.2
F2	22.2 ± 1.2	5.8 ± 0.1
F3	21.7 ± 2.8	5.2 ± 0.5
F4	25.0 ± 1.9	5.0 ± 0.5
F5	28.3 ± 1.2	6.5 ± 0.8
F6	25.5 ± 2.3	5.6 ± 0.6
F7	29.2 ± 2.7	6.2 ± 0.4
F8	30.0 ± 1.2	6.9 ± 0.1
F9	39.4 ± 1.9	6.1 ± 0.2
F10	40.1 ± 4.5	7.0 ± 0.2
F11	35.7 ± 4.1	7.0 ± 0.5
F12	45.9 ± 1.2	6.5 ± 0.2
F13	44.3 ± 2.4	6.8 ± 0.5
F14	48.0 ± 1.8	7.0 ± 0.1

**Data are presented as mean ± SD, n = 3;*

Assurance of stability

The stability assessment of the optimised retinoic acid-loaded nano-transfersome (F12) was conducted under two distinct temperature conditions: 4.0 °C ± 0.2 °C and room temperature, specifically 25-28 °C ± 2 °C, over duration of 3 weeks.[46] The average particle size, percentage of drug content and physical appearance were analysed at the 1st, 2nd and 3rd weeks of storage as shown in Table 6.

The size of the particles in retinoic acid loaded nano-transfersomes increased significantly ($p < 0.05$) during the final week of storage at a temperature range of 25-28 °C ± 2 °C, whereas it remained consistently around 200 nm at refrigerated conditions (4.0 °C ± 0.2 °C). The changes in the size may be due to that the smaller vesicles have the tendency to inclined and dissolve followed by deposit onto larger vesicles, resulting in the growth of the larger ones while the smaller ones vanish. Moreover, nano-vesicular system can aggregate, leading to an increase in their size. This phenomenon is frequently observed at elevated storage temperatures or in the presence of specific ions. Elevated temperatures typically expedite these processes, resulting in more pronounced size alterations.

The retinoic acid content in the F12 formulation did not show a significant decrease throughout the stability study, which lasted up to 3 weeks under both temperature conditions. Additionally, no notable changes were observed in the physical appearance of the retinoic acid-loaded nano-transfersome formulation over the 3-week period, except at the temperature range of 25-28 °C ± 2 °C, where turbidity was noted by the end of the week.

Ocular tolerance assay (HET-CAM irritation test)

Given the delicate nature of the eye, the ocular tolerance test serves as an essential assessment for formulations designed for ocular application. In the HET-CAM irritation test conducted on the CAM of a hen's egg, the irritation potential of 0.05 % retinoic acid loaded nano-transfersome (F12) and the positive control (0.1 N NaOH) was evaluated, followed by the determination of the irritation score expressed in terms of the ocular irritation index (OII). For the eggs treated with the positive control (0.1 N NaOH) solution, the irritation score was recorded at 20.25 ± 1.12, indicating significant irritation characterised by haemorrhage, lysis and coagulation of blood vessels. In contrast, the eggs treated with the optimised retinoic acid loaded nano-transfersome (F12),

Table 6: Characterisation of optimised formulation of nano-transfersomes (F12) for stability studies up to 3 weeks

Characteristic	Time (week)					
	1st		2nd		3rd	
Temperature	4.0 ± 0.2 °C	25-28 ± 2 °C	4.0 ± 0.2 °C	25-28 ± 2 °C	4.0 ± 0.2 °C	25-28 ± 2 °C
Average particle size* (nm)	155.32 ± 4.45	175.56 ± 3.43	165.32 ± 2.49	314.65 ± 4.87	174.35 ± 5.84	358.65 ± 4.99
% DC*	79.12 ± 2.23	78.52 ± 2.40	78.45 ± 2.52	77.95 ± 3.08	78.21 ± 3.70	77.62 ± 4.39
Physical appearance	No significant change	No significant change	No significant change	Slightly turbid	No significant change	Turbid

**Mean ± SD; (n = 3); DC: drug content;*

exhibited an irritation score of 0.5 ± 0.2, thereby confirming that the formulation was non-irritant.

Discussion

By embedding the retinoic acid within the lipid bilayer of nano-transfersome, it is protected from the surrounding aqueous environment, which prevents degradation and preserves its active form. Ultimately, this can aid in the absorption of retinoic acid into ocular cells.[47] The optimisation of the retinoic acid-loaded nano-transfersomes involved adjusting the lipid to surfactant ratio, the volume of ethanol, the concentration of retinoic acid and the duration of stirring, resulting in improved entrapment efficiency and reduced vesicular size with the F12 formulation.

The impact of varying concentrations of phosphatidyl choline and the stirring duration in the orbital shaker during the preparation of nano-transfersomes on particle size was evaluated. An increase in phosphatidyl choline concentration resulted in a corresponding increase in particle size, while the concentration of span-20 remained low and constant. The specific surfactant utilised, such as span-20, has the potential to influence the particle size of the resulting nano-transfersomes. Research indicated that span-20 is associated with smaller particle size. The negatively charged lipid exerts an electrostatic attraction towards the drug, which is anticipated to separate the phospholipid head groups, thereby leading to an increase in particle size.[48]

A significantly high ξ-potential (generally exceeding ± 30 mV) signifies excellent stability and claimed to inhibit the aggregation of nano-transfersomes.[49] This negative charge may assist in overcoming the repulsive negative charges present on the corneal surface, thereby promoting drug penetration and improving delivery to the posterior region of eye.

Increased stirring duration for the preparation of nano-transferosome has improved entrapment efficiency by facilitating effective mixing and interaction among the formulation components, resulting in a more consistent distribution of the retinoic acid within the lipid bilayer. Consequently, this optimises the likelihood of the drug being encapsulated within the nano-transferosomes. Additionally, the deformability properties of nano-transfersomes could improve the penetration of retinoic acid through barriers such as the cornea and sclera. Their exceptional deformability enables them to navigate through tight spaces, rendering them ideal for targeting the posterior segment of the eye.[50]

Findings of kinetic analysis indicated that the different models examined, the Korsmeyer-Peppas model emerged as the best-fitting model, demonstrating the highest degree of correlation coefficient, leading to the conclusion that the extricate action is diffusion-controlled to deliver the drug at posterior region of eye. The notion of ultra-flexibility is based on the ability of vesicles to navigate through ocular barriers and effectively deliver the medication to the posterior segment of the eye without undergoing rupture. TEM imaging has verified that nano-transfersomes successfully passed through pores without collapsing, thereby preserving the encapsulated retinoic acid.

An increase in lecithin concentration correlates with an increase in the viscosity of the retinoic acid-loaded nano-transfersomes.[51] Moreover, the pH levels between 5 and 8 are appropriate for ocular use as this range is deemed non-irritating which was further confirmed by HET-CAM irritation test.[52]

The nano-transfersome formulation loaded with retinoic acid demonstrated an acceptable vesicular size, percentage of retinoic acid content and physical appearance when maintained at temperatures of 4.0 °C ± 0.2 °C and 25-28 °C ± 2 °C over a period of 3 weeks for storage stability analysis.

Conclusion

The present study highlights the significant potential of retinoic acid-loaded nano-transfersomes, which are also referred to as ultra-flexible nanovesicular systems for ocular medicament distribution, particularly for therapy of posterior region of optic diseases such as diabetic retinopathy (DR) and age-related macular degeneration (AMD). The optimisation of retinoic acid-loaded nano-transfersomes was achieved by modifying the formulation

and process parameters, including the lipid to surfactant ratio, ethanol volume, retinoic acid concentration and stirring duration. The impact of the formulation components and their respective concentration on the characteristics of the formulation was assessed in terms of mean vesicle diameter and percentage captured capacity. The optimised F12 composition was reduced to nanoscale, demonstrating a particle size of approximately 155.32 ± 4.45 nm and an entrapment efficiency of 79.12 ± 2.23 %. Additionally, a low PDI of 0.393 for the optimised F12 formulation indicates that the nano-transfersomes have preserved their homogeneity and stability. Moreover, the ξ-potential of -36.5 mV further emphasises excellent stability and is believed to prevent the aggregation of the F12 nano-transfersome formulation. In parallel, *in vitro* drug release studies revealed that approximately 40 % of retinoic acid was released over a 6 h period, demonstrating a prolonged drug release, while nearly 98 % of the medicament was extricate within 24 h. These results suggest that the release mechanism is diffusion-controlled, effectively delivering the drug to the posterior region of the eye, aligning well with the Korsmeyer-Peppas release kinetic model. The F12 formulation exhibited spherical, oval and elongated shapes, resembling multilamellar bilayer vesicles and showcased a consistent system with unique, smooth surfaces and loose aggregates while maintaining integrity. Furthermore, it displayed suitable physicochemical properties such as viscosity and pH for ocular drug delivery, complemented by low ocular irritability potential, high biocompatibility and retention. The nano-transfersome formulation loaded with retinoic acid showed an acceptable vesicular size, percentage of retinoic acid content and physical appearance when stored at temperatures of 4.0 °C ± 0.2 °C and 25-28 °C ± 2 °C over a time period of 3 weeks. In the HET-CAM test, eggs treated with the optimised retinoic acid-loaded nano-transfersome (F12) exhibited an irritation score of 0.5 ± 0.2, confirming that the formulation is non-irritating. Overall, as demonstrated in the HET-CAM assay, the physicochemical parameters and drug entrapment in the nano-transfersome render the composition safe and appropriate for non-invasive drug delivery to the inner eye structures, facilitating access to inner eye tissues. However, ongoing studies such as long-term stability assessments, sterility testing and *in vivo* investigations are essential for a deeper knowing the action and efficacy of the system in delivering the medicament to the posterior region of eye.

Ethics

This study received ethical clearance from the Animal Care and Use Committee (ACUC), Faculty of Veterinary Medicine, Universitas Airlangga. The ethical clearance certificate was issued under the number 2.KEH.2.01.2025, dated 15 January 2025, confirming the study's compliance with ethical standards.

Acknowledgement

None.

Conflicts of interest

The authors declare that there is no conflict of interest.

Funding

This research received no specific grant from any funding agency in the public, commercial, or not-for-profit sectors.

Data access

The data that support the findings of this study are available from the corresponding author upon reasonable individual request.

Author ORCID numbers

Vandana Gupta (VG):
0000-0002-2543-5911

Noopur Srivastava (NS):
0009-0004-8169-9278
Megha Verma (MV):
0000-0002-3550-348X
Mahima Beohar (MB):
0009-0006-1892-6284
Vishal Verma (VV):
0009-0003-7837-3632

Author contributions

Conceptualisation: VG
Methodology: MB, VV
Software: VG, MB
Validation: VG, MV
Formal analysis: NS
Investigation: MV, VG, VV
Resources: VV, MB
Data curation: MJY
Writing –original draft: VG, NS
Writing - review and editing: VG, MV
Visualisation: MB
Supervision: VG
Project administration: VG.

References

1. Marchesi N, Fahmideh F, Boschi F, Pascale A, Barbieri A. Ocular neurodegenerative diseases: interconnection between retina and cortical areas. Cells. 2021 Sep 12;10(9):2394. doi: 10.3390/cells10092394.
2. Varela Fernández R, Díaz Tomé V, Luaces Rodríguez A, Conde Penedo A, García Otero X, Luzardo Álvarez A, et al. Drug delivery to the posterior segment of the eye: biopharmaceutic and pharmacokinetic considerations. Pharmaceutics. 2020 Mar 16;12(3):269. doi: 10.3390/pharmaceutics12030269.
3. Singh P, Gupta V. Curcumin loaded deformable drug carrier for the disease of posterior segment of eye: diabetic retinopathy. Pharma Innov. 2021 Dec 5;10(1):17-21. doi: 10.22271/tpi.2020.v9.i12d.5442.
4. Verma P, Gupta V, Manigauha A. Preparation and characterization of natamycin loaded bioadhesive in situ ophthalmic gel for enhanced bioavailability. J Sustain Mater Process Manag. 2022 Oct 27;2(2):41-7. doi: 10.30880/jsmpm.2022.02.02.006.
5. Thakur SS, Gupta V. Curcumin loaded in situ gel for ocular complication due to diabetes mellitus: dry eye syndrome. Pharma Innov. 2021 Feb 19;10(3):489-492.
6. Park SJ, Park DH. Revisiting lipids in retinal diseases: a focused review on age related macular degeneration and diabetic retinopathy. J Lipid Atheroscler. 2020 Sep 18;9(3):406-420. doi: 10.12997/jla.2020.9.3.406.
7. Zhang Y, Wang Y, Jin Q, Wang Q, Yang Y, Yu X, et al. The association between diabetic retinopathy and the prevalence of age related macular degeneration—The Kailuan Eye Study. Front Public Health. 2022 Jul 18;10:922289. doi: 10.3389/fpubh.2022.922289.
8. Stahl A. The diagnosis and treatment of age related macular degeneration. Dtsch Arztebl Int. 2020 Jul 20;117(29-30):513-22. doi: 10.3238/arztebl.2020.0513.
9. Schofield D, Kraindler J, Tan O, Shrestha R, Jelovic D, West S, et al. Patient reported health related quality of life in individuals with inherited retinal diseases. Ophthalmol Sci. 2022 Mar;2(1):100106. doi: 10.1016/j.xops.2021.100106.
10. Dammak A, Huete Toral F, Carpena Torres C, Martin Gil A, Pastrana C, Carracedo G. From oxidative stress to inflammation in the posterior ocular diseases: diagnosis and treatment. Pharmaceutics. 2021 Aug 31;13(9):1376. doi: 10.3390/pharmaceutics13091376.
11. Gabai A, Zeppieri M, Finocchio L, Salati C. Innovative strategies for drug delivery to the ocular posterior segment. Pharmaceutics. 2023 Jul 1;15(7):1862. doi: 10.3390/pharmaceutics15071862.
12. Gupta V, Trivedi P. Dermal drug delivery for cutaneous malignancies: literature at a glance. J Pharm Innov. 2016 Mar;11:1-33. doi: 10.1007/s12247-015-9236-3.
13. Bisen AC, Dubey A, Agrawal S, Biswas A, Rawat KS, Srivastava S, et al. Recent updates on ocular disease management with ophthalmic ointments. Ther Deliv. 2024 Jun 2;15(6):463-80. doi: 10.1080/20415990.2024.2346047.
14. Qi Q, Wei Y, Zhang X, Guan J, Mao S. Challenges and strategies for ocular posterior diseases therapy via non invasive advanced drug delivery. J Control Release. 2023 Sep 1;361:191-211. doi: 10.1016/j.jconrel.2023.07.055.
15. Gupta V, Sanyogita KM, Manigauha A. Novel formulation of aloe vera and quercetin in the management of dermal disease: eczema. J Pharm Drug Res. 2021;4(2):480-7. doi: 10.13140/RG.2.2.21014.27207.
16. Wu Y, Li X, Fu X, Huang X, Zhang S, Zhao N, et al. Innovative nanotechnology in drug delivery systems for advanced treatment of posterior segment ocular diseases. Adv Sci. 2024 Aug;11(32):2403399. doi: 10.1002/advs.202403399.
17. Seema S, Chand SG, Ashish M, Vandana G. Ultra flexible nanocarrier for enhanced the ocular delivery of quercetin in management of macular edema. Educ Soc Human Stud. 2022;3(1):9-26. doi: 10.22158/eshs.v3n1p9.
18. Srivastava V, Singh V, Khatri DK, Mehra NK. Recent trends and updates on ultradeformable and elastic vesicles in ocular drug delivery. Drug Discov Today. 2023 Aug 1;28(8):103647. doi: 10.1016/j.drudis.2023.103647.
19. Gupta V, Trivedi P. In vitro and in vivo characterization of pharmaceutical topical nanocarriers containing anticancer drugs for skin cancer treatment. In: Grumezescu AM, editor. Lipid Nanocarriers for Drug Targeting. William Andrew; 2018. p.563-627. doi: 10.1016/B978-0-12-813687-4.00015-3.
20. Gupta V, Chuttani K, Mishra AK, Trivedi P. Topical delivery of fluorescence (6 Cf) labeled and radiolabeled (99m Tc) cisplatin and imiquimod by a dual drug delivery system. J Label Compd Radiopharm. 2014 May;57(6):425-33. doi: 10.1002/jlcr.3201.
21. Xu C, Wu Y, Zhao L, Zhou W, Li Y, Yi X, et al. Transdermal hormone delivery: strategies, application and modality selection. J Drug Deliv Sci Technol. 2023 Sep 1;86:104730.
22. Kumar L, Rana R, Kukreti G, Aggarwal V, Chaurasia H, Sharma P, et al. Overview of spanlastics: a groundbreaking elastic medication delivery device with versatile

prospects for administration via various routes. Curr Pharm Des. 2024 Aug 1;30(28):2206-21. doi: 10.2174/0113816128313398240613063019.
23. Peña Rodríguez E, Moreno MC, Blanco Fernandez B, González J, Fernández Campos F. Epidermal delivery of retinyl palmitate loaded transfersomes: penetration and biodistribution studies. Pharmaceutics. 2020 Jan 30;12(2):112. doi: 10.3390/pharmaceutics12020112.
24. Ranganath SH, Thanuja MY, Anupama C, Manjunatha TD. Systemic drug delivery to the posterior segment of the eye: overcoming blood–retinal barrier through smart drug design and nanotechnology. In: Immobilization Strategies: Biomedical, Bioengineering and Environmental Applications. 2021. p.219-269. doi: 10.1007/978-981-15-7998-1_6.
25. Motwani K, Gupta V. Nano transfersomes of vitamin E and aloe vera for the management of psoriasis: nano transfersomes for the management of psoriasis. J Sustain Mater Process Manag. 2022 Oct 27;2(2):9-18. doi: 0.30880/jsmpm.0000.00.00.000.
26. Saini N, Gupta V. Eutectic mixture: solvent in the development of biocompatible liposome to manage dermatitis. Curr Cell Sci. 2025 May 14;1(1):1-10. doi: 10.2174/0127726215370113250509055809.
27. Gun'ko VM, Klyueva AV, Levchuk YN, Leboda R. Photon correlation spectroscopy investigations of proteins. Adv Colloid Interface Sci. 2003 Sep 18;105(1-3):201-328. doi: 10.1016/S0001-8686(03)00091-5.
28. Jamadar AT, Peram MR, Chandrasekhar N, Kanshide A, Kumbar VM, Diwan PV. Formulation, optimization, and evaluation of ultradeformable nanovesicles for effective topical delivery of hydroquinone. J Pharm Innov. 2023 Jun;18(2):506-24. doi: 10.1007/s12247-022-09657-7.
29. Gupta PK, Pancholi SS, Das P. In vitro drug release testing method for nepafenac ophthalmic suspension. J Pharm Sci. 2024 Apr;113(4):1061-7. doi: 10.1016/j.xphs.2023.11.028.
30. Bohrey S, Chourasiya V, Pandey A. Polymeric nanoparticles containing diazepam: preparation, optimization, characterization, in vitro drug release and release kinetic study. Nano Converg. 2016 Mar 1;3(1):3. doi: 10.1186/s40580-016-0061-2.
31. Kumari S, Nehra A, Gupta K, Puri A, Kumar V, Singh KP, Kumar M, Sharma A. Chlorambucil loaded graphene oxide based nano vesicles for cancer therapy. Pharmaceutics. 2023 Feb 15;15(2):649. doi: 10.3390/pharmaceutics15020649.
32. Wang W, Shu GF, Lu KJ, Xu XL, Sun MC, Qi J, et al. Flexible liposomal gel dual loaded with all trans retinoic acid and betamethasone for enhanced therapeutic efficiency of psoriasis. J Nanobiotechnol. 2020 Dec;18:182. doi: 10.1186/s12951-020-00635-0.
33. Apolinário AC, Naser YA, Volpe Zanutto F, Vora LK, Sabri AH, Li M, et al. Novel lipid nanovesicle loaded dissolving microarray patches for fenretinide in breast cancer chemoprevention. J Control Release. 2024 Oct 1;374:76-88. doi: 10.1016/j.jconrel.2024.07.080.
34. Gupta V, Trivedi P. Enhancement of storage stability of cisplatin loaded protransfersome topical drug delivery system by surface modification with block copolymer and gelling agent. J Drug Deliv Sci Technol. 2012 Jan;22(4):361-6. doi: 10.1016/S1773-2247(12)50060-2.
35. Vieira LM, Silva RS, da Silva CC, Presgrave OA, Boas MH. Comparison of the different protocols of the hen's egg test chorioallantoic membrane (HET CAM) by evaluating the eye irritation potential of surfactants. Tox In Vitro. 2022 Feb;78:105255. doi: 10.1016/j.tiv.2021.105255.
36. Yozgatlı V, Üstündağ Okur N, Okur ME, Sipahi H, Charehsaz M, Aydın A, et al. Managing allergic conjunctivitis via ophthalmic microemulsions: formulation, characterization, in vitro irritation studies based on EpiOcular™ eye irritation assay and in vivo studies in rabbit eye. J Surfact Deterg. 2023 Nov;26(6):853-66. doi: 10.1002/jsde.12691.
37. Simrah, Hafeez A, Usmani SA, Izhar MP. Transfersome, an ultra deformable lipid based drug nanocarrier: an updated review with therapeutic applications. Naunyn Schmiedeberg Arch Pharmacol. 2024 Feb;397(2):639-73. doi: 10.1007/s00210-023-02670-8.
38. Su D, Wang X, Liu X, Miao J, Zhang Z, Zhang Y, et a. A comprehensive study of the colloidal properties, biocompatibility, and synergistic antioxidant actions of Antarctic krill phospholipids. Food Chem. 2024 Sep 1;451:139469. doi: 10.1016/j.foodchem.2024.139469.
39. Dmour I. Absorption enhancement strategies in chitosan based nanosystems and hydrogels intended for ocular delivery: latest advances for optimization of drug permeation. Carbohydr Polym. 2024 Jul 15;320:122486. doi: 10.1016/j.carbpol.2024.122486.
40. Bandyopadhyay P. Fatty alcohols or fatty acids as niosomal hybrid carrier: effect on vesicle size, encapsulation efficiency and in vitro dye release. Colloids Surf B Biointerfaces. 2007 Jul 1;58(1):68-71. doi: 10.1016/j.colsurfb.2007.01.014.
41. Petersson K, Ilver D, Johansson C, Krozer A. Brownian motion of aggregating nanoparticles studied by photon correlation spectroscopy and measurements of dynamic magnetic properties. Anal Chim Acta. 2006 Jul 28;573:138-46. doi: 10.1016/j.aca.2006.03.055.
42. Mirza R, Shah KU, Khan AU, Fawad M, Rehman AU, Ahmed N, et al. Statistical design and optimization of nano transfersomes based chitosan gel for transdermal delivery of cefepime. Drug Dev Ind Pharm. 2024 Jun;50(6):511-23. doi: 10.1080/03639045.2024.2353098.
43. Barzegar Jalali M. Kinetic analysis of drug release from nanoparticles. J Pharm Pharm Sci. 2008 May 7;11(1):167-77. doi: 10.18433/j3d59t.
44. Petropoulos JH, Papadokostaki KG, Sanopoulou M. Higuchi's equation and beyond: overview of the formulation and application of a generalized model of drug release from polymeric matrices. Int J Pharm. 2012 Nov 1;437(1-2):178-91. doi: 10.1016/j.ijpharm.2012.08.012.
45. Askarizadeh M, Esfandiari N, Honarvar B, Sajadian SA, Azdarpour A. Kinetic modeling to explain the release of medicine from drug delivery systems. ChemBioEng Rev. 2023 Dec;10(6):1006-49. doi: 10.1002/cben.202300027.
46. Lemoine D, Francois C, Kedzierewicz F, Préat V, Hoffmann M, Maincent P. Stability study of nanoparticles of poly(ε-caprolactone), poly(d,l lactide) and poly(d,l lactide co glycolide). Biomaterials. 1996 Nov 1;17(22):2191-7. doi: 10.1016/0142-9612(96)00049-X.
47. Dragicevic N, Maibach HI. Liposomes and other nanocarriers for the treatment of acne vulgaris: improved therapeutic efficacy and skin tolerability. Pharmaceutics. 2024 Feb 22;16(3):309. doi: 10.3390/pharmaceutics16030309.
48. Paramshetti S, Angolkar M, Talath S, Osmani RA, Spandana A, Al Fatease A, et al. Unravelling the in vivo dynamics of liposomes: insights into biodistribution

and cellular membrane interactions. Life Sci. 2024 Apr;322:122616. doi: 10.1016/j.lfs.2024.122616.
49. Rafique M, Ali Z, Sohail S, Zahid F, Khan MI, ud Din F, et al. Development of dexibuprofen loaded nano transfersomal gel with enhanced biopharmaceutical performance in complete Freund's adjuvant induced arthritis model. J Drug Deliv Sci Technol. 2024 Sep 1;98:105928. doi: 10.1016/j.jddst.2024.105928.
50. Chandel A, Kandav G. Insights into ocular therapeutics: a comprehensive review of anatomy, barriers, diseases and nanoscale formulations for targeted drug delivery. J Drug Deliv Sci Technol. 2024 May;79:105785. doi: 10.1016/j.jddst.2024.105785.
51. Zewail M, Abbas H, Ali ME, Makled S. Melatonin hyalurosomes as a powerful antioxidant for combating skin damage induced by UV radiation. J Liposome Res. 2025 Apr;1-6. doi: 10.1080/08982104.2025.2484732.
52. Pal Kaur I, Kanwar M. Ocular preparations: the formulation approach. Drug Dev Ind Pharm. 2002 Jan;28(5):473-93. doi: 10.1081/DDC-120003445.